

**1 The role of vertical eddy flux in Southern Ocean heat**  
**2 uptake**

A. K. Morrison<sup>1</sup>, O. A. Saenko<sup>2,3</sup>, A. McC. Hogg<sup>1</sup> and P. Spence<sup>3</sup>

---

Corresponding author: Adele Morrison, Research School of Earth Sciences, Australian National University, Canberra, ACT 0200, Australia. (adelem@princeton.edu)

<sup>1</sup>ARC Centre of Excellence for Climate System Science and Research School of Earth Sciences, Australian National University, Canberra, Australian Capital Territory, Australia.

<sup>2</sup>Canadian Centre for Climate Modelling and Analysis, Environment Canada, Victoria, British Columbia, Canada.

<sup>3</sup>ARC Centre of Excellence for Climate System Science and Climate Change Research Centre, University of New South Wales, Sydney, New South Wales, Australia.

3 The role of changing vertical eddy heat flux on Southern Ocean heat up-  
4 take is investigated in an idealised eddy-permitting ocean model. Enhanced  
5 air-sea heat flux drives deep-reaching southern warming, due to a reduction  
6 in the isopycnal meridional temperature gradient and therefore decreased up-  
7 ward eddy heat flux. This mechanism is qualitatively similar in models with  
8 either permitted or parameterised eddies, due to its dependence on the isopy-  
9 cnal temperature gradient rather than the dynamical response of the eddy  
10 field. In contrast, increased wind stress drives mid-depth Southern Ocean cool-  
11 ing through an enhancement of the eddy field and resultant eddy heat di-  
12 vergence. The transient cooling extends over multiple decades while the mean  
13 flow adjusts to balance the faster eddy response. This wind-driven cooling  
14 mechanism has not been captured by coarse resolution models with fixed eddy  
15 parameterisations and is a possible candidate for the recent cooling observed  
16 in the Southern Ocean.

## 1. Introduction

17 The oceans account for an overwhelming proportion ( $\sim 93\%$ ) of the warming of the earth  
18 system over the past fifty years [*Levitus et al.*, 2012], and a large fraction of that ocean heat  
19 uptake has occurred in the upper 2000 m of the midlatitude Southern Ocean [*Gille*, 2008].  
20 The intensified Southern Ocean warming has likely been driven by some component of  
21 the changing local surface forcing; a positive trend in the Southern Annular Mode has en-  
22 hanced and shifted the westerly winds southward [*Thompson and Solomon*, 2002], surface  
23 air temperatures have increased [*Chapman and Walsh*, 2007] and evidence points towards  
24 increased precipitation over far southern latitudes due to an amplified hydrological cycle  
25 [*Durack et al.*, 2012]. Yet the relative importance of the different forcing components  
26 and the mechanisms by which they may cause deep-reaching southern warming are un-  
27 clear, due to a combination of limited observations, uncertain atmospheric forcing and  
28 insufficient modelling resolution.

29 *Meijers et al.* [2011] divided the Southern Ocean temperature trend into an adiabatic  
30 component due to a wind-driven poleward migration of the Antarctic Circumpolar Current  
31 [as suggested by *Gille*, 2008] and a diabatic component due to changes in the vertical flux  
32 of heat from the surface and between ocean layers. The adiabatic component contributes  
33 a large warming trend, while the diabatic component contributes an opposing cooling  
34 trend, which acts to reduce the adiabatic trend by approximately half to produce the net  
35 observed deep warming. *Meijers et al.* [2011] do not attribute the cause of the diabatic  
36 cooling. Our aim in this paper is to investigate the dynamics of heat uptake processes

37 which may be contributing to the diabatic trend in the Southern Ocean and in particular  
38 the role of eddies in modifying ocean temperature trends.

39 The ocean heat content trend arising from diabatic processes will be reflected in changes  
40 in the time mean vertical heat flux budget. Numerical modelling studies have found that  
41 below the surface mixed layer, the globally averaged vertical flux of heat is primarily a  
42 balance between the wind-driven mean circulation pumping heat downwards and eddies  
43 (permitted or parameterised) transporting heat upwards along isopycnals [*Gregory*, 2000;  
44 *Wolfe et al.*, 2008]. It is reasonable to expect that eddies transport buoyancy (i.e. heat)  
45 upwards in the global integral, because the baroclinic instability process acts to reduce  
46 available potential energy. Both the mean and eddy terms in the vertical heat flux budget  
47 are dominated by contributions from the Southern Ocean. Downward flux of heat by  
48 vertical diffusion in the tropics is only significant in the global budget in the upper few  
49 hundred metres of the ocean.

50 Two main mechanisms for Southern Ocean heat uptake have been proposed - one driven  
51 by increased atmospheric surface temperature and the other by enhanced westerly winds.  
52 In the first mechanism, warming is amplified at mid-depths due to a reduced along-  
53 isopycnal meridional temperature gradient in a warmer climate and therefore decreased  
54 upward eddy heat flux, as shown in a coarse resolution model with parameterised isopycnal  
55 diffusion by *Gregory* [2000]. *Huang et al.* [2003] looked at the sensitivity of deep ocean  
56 heat uptake to a range of surface forcing and diffusivity perturbations and concluded  
57 that the large variation in deep ocean heat uptake between models arises primarily due  
58 to the high sensitivity to parameterised isopycnal diffusivity in the Southern Ocean and

59 diapycnal diffusivity in the tropics. *Brierley et al.* [2008], in another coarse resolution  
60 coupled model study, found that reduced isopycnal diffusion was the largest contributor  
61 to the global imbalance leading to the warming trend between 350-1500 m.

62 Despite the dependence of this Southern Ocean warming mechanism on the eddy field,  
63 it has been largely untested in eddy-permitting or eddy-resolving models. *Wolfe and*  
64 *Cessi* [2009] investigated ocean heat uptake in an idealised eddy-resolving simulation  
65 with a northern hemisphere surface warming perturbation. In agreement with the coarse  
66 resolution study of *Gregory* [2000], the northern surface temperature gradient decreased  
67 in the warmer climate, reducing the vertical eddy heat flux and resulting in deep ocean  
68 heat uptake. However in their model, density was a linear function of temperature only.  
69 With no isopycnal temperature gradient, the only mechanism available for eddies to alter  
70 the vertical heat budget is through a change in the potential energy that maintains the  
71 eddy activity. Whether the Southern Ocean vertical eddy heat flux decreases in response  
72 to surface warming due to a change in baroclinicity or due to a change in the isopycnal  
73 temperature gradient remains to be tested in an eddy-permitting or eddy-resolving model.

74 The second proposed mechanism for Southern Ocean heat uptake acts through a wind-  
75 driven enhancement of the downward mean heat flux and is the primary cause of Southern  
76 Ocean warming in the Third Coupled Model Intercomparison Project (CMIP3) twentieth-  
77 century experiments [*Cai et al.*, 2010]. However, none of the CMIP3 models resolve eddies  
78 and are therefore missing the response of the eddy heat flux to changing wind stress [*Hogg*  
79 *et al.*, 2008], which may significantly offset the wind-driven heat uptake. In this paper,  
80 we use a suite of wind stress and surface warming perturbations in an idealised eddy-

81 permitting model to explore the role of the Southern Ocean eddy field on these two  
82 mechanisms of deep ocean heat uptake.

## 2. Numerical Model

83 We use an idealised,  $1/4^\circ$  eddy-permitting ocean sector configuration of the MITgcm  
84 [Marshall *et al.*, 1997], with an experimental setup identical to that described in Hogg  
85 *et al.* [2013]. We refer the reader to Figure 1 of that paper for an illustration of the  
86 model bathymetry and surface forcing for the reference case. The model domain is a  $40^\circ$   
87 wide sector, extending from  $70^\circ\text{S}$  to  $70^\circ\text{N}$ , with a southern reentrant channel containing  
88 a simple Drake Passage-like sill of depth 1800 m. Vertical resolution increases towards  
89 the surface over 36 vertical levels. The model is run in hydrostatic, Boussinesq mode,  
90 and no explicit eddy parameterisation scheme is used. Horizontal viscosity/diffusion are  
91 minimised with a biharmonic lateral viscosity/diffusivity of  $10^{11} \text{ m}^4 \text{ s}^{-1}$ . Background  
92 vertical diffusion is set to  $10^{-5} \text{ m}^2 \text{ s}^{-1}$ , with a surface enhancement in the upper 300 m  
93 to generate appropriate mixed layer depths. The convective adjustment scheme also  
94 amplifies the background vertical diffusivity to remove unstable density profiles. A linear  
95 equation of state is employed, with both temperature and salinity dependence. The surface  
96 forcing is temporally invariant and zonally uniform, with prescribed wind stress, surface  
97 temperature relaxation and a fixed freshwater flux (see Hogg *et al.* [2013]). The model is  
98 close to equilibrium after a spinup period of 2500 years, after which point perturbations  
99 are split off from the reference case and run for a further 100 years. The forcing undergoes  
100 a step change and is then kept steady in the new perturbed configuration for the entire  
101 100 years. In the warming perturbations, the surface relaxation temperature is increased

102 uniformly across the domain by 0.5°C, 1°C, 2°C or 4°C as specified in the analysis. For  
 103 the wind stress perturbations, the prescribed wind stress south of 30°S is scaled by factors  
 104 of 0.7, 1.2, 1.3 and 2, as specified in the analysis. There is only minimal feedback between  
 105 wind stress changes and local surface heat fluxes, meaning that we can easily separate the  
 106 wind- and warming-induced changes.

### 3. Mean Vertical Heat Flux

107 Vertical heat fluxes are calculated following *Wolfe et al.* [2008]. The time-mean heat  
 108 budget is separated into the sum of the heat content tendency ( $\mathcal{T}$ ), advective heat fluxes  
 109 due to the mean flow ( $\mathcal{M}$ ) and eddies ( $\mathcal{E}$ ), and heat fluxes arising from parameterised  
 110 sub-grid-scale processes ( $\mathcal{P}$ ; including turbulent diffusion and convective adjustment), as  
 111 follows:

$$112 \quad \mathcal{T} + \mathcal{M} + \mathcal{E} + \mathcal{P} = 0. \quad (1)$$

113 If we integrate from the bottom  $-H$  to a reference level  $z_o$  and over a horizontal subdomain  
 114  $\mathcal{A}$  (with boundary  $\partial\mathcal{A}$ ), the first three terms are calculated as

$$115 \quad \mathcal{T} = \rho_o c_p \int_{-H}^{z_o} \int_{\mathcal{A}} \frac{\Delta\theta}{\Delta t} dA dz \quad (2)$$

$$116 \quad \mathcal{M} = \rho_o c_p \left( \int_{\mathcal{A}} \overline{w\theta}(z_o) dA + \int_{-H}^{z_o} \oint_{\partial\mathcal{A}} \overline{u_H\theta} d\sigma dz \right) \quad (3)$$

$$117 \quad \mathcal{E} = \rho_o c_p \left( \int_{\mathcal{A}} \overline{w'\theta'}(z_o) dA + \int_{-H}^{z_o} \oint_{\partial\mathcal{A}} \overline{u'_H\theta'} d\sigma dz \right) \quad (4)$$

120 where  $c_p$  is the specific heat content,  $\theta$  is potential temperature,  $u_H$  is the horizontal  
 121 component of velocity normal to the boundary,  $\bar{\cdot}$  is the temporal average over the time  
 122 period  $\Delta t$  and primed quantities indicate deviations from the temporal mean.  $dA$  is the  
 123 differential area of the subdomain  $\mathcal{A}$ , while  $d\sigma$  is the differential length along its boundary

124  $\partial\mathcal{A}$ . The second term in Equations 3 and 4 represents the heat flux through the lateral  
125 boundary of the subdomain. The sub-gridscale term,  $\mathcal{P}$ , is not calculated explicitly, but  
126 rather as the residual of the first three terms in Equation 1. The sign of  $\mathcal{P}$  indicates  
127 whether convective or diffusive fluxes are dominating the sub-gridscale term; in the polar  
128 regions, convection dominates and  $\mathcal{P}$  is positive, indicating upward heat flux, while in the  
129 tropics, vertical diffusion dominates and  $\mathcal{P}$  is negative, indicating downward heat flux.

130 The vertical heat flux components for the reference case simulation, averaged over the  
131 entire domain, are shown in Figure 1a. Figures 1b-d show the ‘vertical’ heat flux (actually  
132 the net divergence, including the lateral terms in Equations 3 and 4) for three subdomains,  
133 divided according to the sign of the mean heat flux, following *Wolfe and Cessi* [2009].  
134 At mid-depth ( $\sim 300$ – $2000$  m) and averaged over the entire domain, the primary balance  
135 is between downward heat flux by the mean flow and upward heat flux by eddies, both  
136 dominated by contributions from the Southern Ocean (Figure 1b) and consistent with the  
137 previous studies of *Gregory* [2000] and *Wolfe et al.* [2008]. The magnitude of the eddy heat  
138 flux is close to that in the eddy-resolving MITgcm model analysed in *Wolfe et al.* [2008];  
139 the area-averaged mid-depth eddy flux in our eddy-permitting model is 20% less than in  
140 their higher resolution model. In the upper ocean, where the model has increased vertical  
141 diffusivity (above 300 m), the primary global balance is between downward diffusive heat  
142 flux from the tropics and upward heat flux by Southern Ocean eddies. Since we are  
143 primarily interested in the response of the vertical heat fluxes to forcing changes, we refer  
144 the reader to *Wolfe et al.* [2008] for a more in-depth explanation and regional analysis of  
145 the time mean vertical heat flux.



## 4. Response to Idealised Climate Change Scenarios

### 4.1. Surface Warming

146 We first consider the response to a uniform  $+2^{\circ}\text{C}$  surface warming perturbation. The  
147 ocean warms (i.e.  $\mathcal{T} > 0$ ) due to changes in each of the mean, eddy and sub-gridscale  
148 vertical heat fluxes (solid lines in Figure 2a). The large warming in the upper 300 m  
149 is concentrated in the tropics (not shown) and arises from both increased downward  
150 diffusive heat flux and decreased upward mean heat flux. At mid-depths ( $\sim 300\text{-}2000$  m),  
151 a significant fraction of the heat uptake occurs in the southern region (dashed lines in  
152 Figure 2a) and is predominantly due to a decrease in the upward eddy heat flux, consistent  
153 with the atmospheric warming driven mechanism identified in previous coarse resolution  
154 studies with parameterised eddies [*Gregory, 2000; Huang et al., 2003; Brierley et al., 2008*].  
155 As time progresses over the 100 years of the warming perturbation, the anomalous vertical  
156 eddy heat flux remains the dominant cause of heat uptake in the global integral in the  
157 depth range 300-1000 m, and the dominant cause of heat uptake in the southern region  
158 down to 2000 m. Below 1000 m in the global integral, the change in the mean vertical  
159 heat flux becomes increasingly significant in the heat uptake over the first century. The  
160 response is qualitatively similar for warming perturbations of different magnitudes.

161 The upward eddy heat flux in the mid-depth southern region scales inversely with the  
162 magnitude of the surface warming perturbation (Figure 2b). In the Southern Ocean,  
163 eddies flux heat along tilted isopycnals and the vertical eddy heat flux shown in Figure 2a  
164 is actually the vertical component of the along-isopycnal heat flux. **Strong precipitation**  
165 **over the Southern Ocean leads to surface waters that are fresher than deep waters. Con-**  
166 **sidered on an isopycnal, this salinity gradient necessitates a negative along-isopycnal tem-**

167 perature gradient (i.e. colder surface waters), since these quantities must compensate, to  
168 first order, on an isopycnal. Assuming downgradient, along-isopycnal tracer diffusion [e.g.  
169 *Redi*, 1982] of the form  $\overline{v'\theta'^\rho} = -\kappa\overline{\theta_y^\rho}$  (where  $(\cdot)^\rho$  indicates we are using an isopycnal  
170 framework), it is possible to trace the cause of the reduced upward eddy heat flux and  
171 hence the mid-depth warming in the southern region to the change in the along-isopycnal  
172 meridional temperature gradient (Figure 2c). In agreement with the coarse resolution  
173 study of *Gregory* [2000], the upward eddy heat flux in the southern region decreases due  
174 to faster warming in the surface region than at depth and a consequent reduction in the  
175 rate of along-isopycnal eddy mixing of temperature. The isopycnal temperature gradient  
176 across southern latitudes decreases as the surface relaxation temperature is increased,  
177 scaling similarly to the vertical eddy heat flux (Figure 2b).

## 4.2. Enhanced Southern Wind Stress

178 Previous Southern Ocean observational and modelling studies have found a fast (2-3  
179 year) and approximately linear response of the eddy kinetic energy to increasing wind  
180 stress [e.g. *Meredith and Hogg*, 2006; *Hogg et al.*, 2008]. The enhancement of the eddy  
181 field with wind stress is a release of available potential energy, leading to an increase in  
182 the upward vertical eddy heat flux in the southern region (Figure 3a). This is the oppo-  
183 site response compared with the surface warming perturbation described in Section 4.1  
184 (Figure 2a). The mean vertical downward heat flux associated with the upper overturning  
185 cell acts to deepen isopycnals on the northern side of the circumpolar current and thereby  
186 to warm at mid-depth; the timescale for this process is advective and therefore slower  
187 than the eddy response. Although we refer to the ‘vertical’ mean and eddy heat fluxes in

188 the southern region, these include significant contributions from lateral fluxes across the  
189 subdomain boundary at 40°S. Figure 3b shows the separation of the net heat divergence  
190 into the true vertical and lateral components.

191 The net result of the mean and eddy responses is a small transient cooling trend in  
192 the mid-depth levels of the southern region. The cooling continues for around 60 years,  
193 until the mean flow increases sufficiently to balance the change in the eddy flux. Despite  
194 minimal change in the local surface heat flux, cooling is able to extend throughout the  
195 water column due to changes in the lateral components of the mean and eddy heat fluxes  
196 (shown in Figure 3b). Analysis of a range of wind stress perturbations indicates a near  
197 one-to-one relationship between the mid-depth eddy heat flux and the prescribed wind  
198 stress (Figure 3c). In contrast to the surface warming perturbations, the along-isopycnal  
199 temperature gradient remains approximately constant for small ( $\sim \pm 30\%$ ) wind stress  
200 perturbations (Figure 3d). The change in eddy heat flux is instead driven by increased  
201 baroclinicity (i.e. the eddy heat flux scales with the eddy kinetic energy). Although the  
202 mid-depth southern region cools following the change in wind forcing, the net heat uptake  
203 integrated over the entire domain is positive (not shown), due to a reduction in the mean  
204 upward heat flux in the tropics.

### 4.3. Combined Warming and Enhanced Wind Stress

205 The response of the vertical eddy heat flux to a wind stress perturbation (Figure 3c)  
206 has the opposite sign compared with the response to a warming perturbation (Figure 2b).  
207 If the two perturbation responses were to combine in an approximately linear way, the  
208 increase in westerly winds could partially reduce surface heat flux-driven warming in the

209 mid-depth Southern Ocean. To explore this possibility, we have run a combined surface  
210 warming (uniform  $+2^{\circ}\text{C}$ ) and enhanced southern wind stress ( $1.3 \times \tau_o$ ) perturbation ex-  
211 periment. As would be expected from the linear sum of the separate warming and wind  
212 stress experiments, the net heat uptake integrated over the entire domain is larger in the  
213 combined perturbation than in either of the independent perturbations. However, in the  
214 southern region, the addition of the enhanced wind stress to the warming perturbation  
215 results in a small decrease in the heat uptake, compared with the surface warming only  
216 perturbation (not shown); this mechanism may account for the observed recent cooling  
217 in the mid-depth Southern Ocean that was inferred to be due to diabatic processes [*Mei-*  
218 *jers et al.*, 2011]. The southern region heat uptake is reduced for a period of  $\sim 60$  years,  
219 while the mean flow adjusts to the increased wind stress. After the mean heat flux has  
220 adjusted to balance the change in the eddy heat flux, the rate of heat uptake matches that  
221 in the warming only perturbation. The cumulative heat uptake in the southern region,  
222 integrated over full depth, is reduced by 5% over the 100 years of simulation.

## 5. Discussion and Conclusions

223 We have used an eddy-permitting numerical model to investigate two mechanisms of  
224 mid-depth Southern Ocean temperature change, both of which rely on changes in the ver-  
225 tical eddy heat flux. The first mechanism, driven by increased surface heat flux and iden-  
226 tified in a coarse resolution model by *Gregory* [2000], causes mid-depth warming through  
227 a reduction in the upward eddy heat flux. In a warmer climate, the along-isopycnal  
228 meridional temperature gradient decreases, leading to reduced isopycnal diffusion of tem-  
229 perature. Since the mechanism does not depend on a change in the eddy field, the response

230 of the vertical eddy heat flux in our eddy-permitting model is qualitatively similar to that  
231 found in coarse resolution simulations with parameterised isopycnal diffusion.

232 The second mechanism involves a response to increased wind stress forcing, which causes  
233 a transient cooling in the mid-depth southern region due to the faster response of the  
234 vertical eddy heat flux compared with the vertical mean heat flux. The upward eddy heat  
235 flux scales with the eddy kinetic energy and therefore responds on a timescale of 2-3 years,  
236 while the downward mean heat flux changes on the timescale for the adjustment of the  
237 upper overturning circulation, which in our model is  $\sim 60$  years. During this adjustment, a  
238 transient cooling occurs in the mid-depth southern region. Note that the relation between  
239 the mean and eddy components in the Southern Ocean vertical heat budget is quite  
240 different to that in the overturning circulation; at equilibrium, the vertical eddy heat flux  
241 nearly exactly opposes the vertical mean heat flux (Figure 1b), while the mean component  
242 of the overturning is significantly larger than the eddy component of the overturning  
243 [*Morrison and Hogg, 2013*]. Unlike in the surface warming mechanism, the response of  
244 the vertical eddy heat flux to enhanced wind stress may differ greatly between coarse  
245 resolution and eddy-permitting or eddy-resolving models. Indeed, in the CMIP3 models,  
246 enhanced wind stress drives Southern Ocean warming, rather than cooling, due to the  
247 unresponsive eddy parameterisations in these coarse resolution models [*Cai et al., 2010*].

248 **Acknowledgments.** AMH was supported by Australian Research Council Future Fel-  
249 lowship FT120100842. The numerical model was run on the NCI National Facility in  
250 Canberra, Australia, which is supported by the Australian Commonwealth Government.

## References

- 251 Brierley, C. M., M. Collins, and A. J. Thorpe (2008), The impact of perturbations to  
252 ocean-model parameters on climate and climate change in a coupled model, *Clim. Dyn.*,  
253 *34*, 325–343.
- 254 Cai, W., T. Cowan, S. Godfrey, and S. Wijffels (2010), Simulations of processes associated  
255 with the fast warming rate of the southern midlatitude ocean, *J. Clim.*, *23*, 197–206.
- 256 Chapman, W. L., and J. E. Walsh (2007), A synthesis of Antarctic temperatures, *J. Clim.*,  
257 *20*, 4096–4117.
- 258 Durack, P. J., S. E. Wijffels, and R. J. Matear (2012), Ocean salinities reveal strong global  
259 water cycle intensification during 1950 to 2000, *Science*, *336*, 455–458.
- 260 Gille, S. T. (2008), Decadal-scale temperature trends in the Southern Hemisphere ocean,  
261 *J. Clim.*, *21*, 4749–4765.
- 262 Gregory, J. M. (2000), Vertical heat transports in the ocean and their effect on time-  
263 dependent climate change, *Clim. Dyn.*, *16*, 501–515.
- 264 Hogg, A. McC., M. P. Meredith, J. R. Blundell, and C. Wilson (2008), Eddy heat flux in  
265 the Southern Ocean: Response to variable wind forcing, *J. Clim.*, *21*, 608–620.
- 266 Hogg, A. McC., H. A. Dijkstra, and J. A. Saenz (2013), The energetics of a  
267 collapsing meridional overturning circulation, *J. Phys. Oceanogr.*, *43*, 1512–1524,  
268 doi:10.1175/JPO-D-12-0212.1.
- 269 Huang, B., P. H. Stone, and C. Hill (2003), Sensitivities of deep-ocean heat uptake and  
270 heat content to surface fluxes and subgrid-scale parameters in an ocean general circu-  
271 lation model with idealized geometry, *J. Geophys. Res.*, *108*, C13,015.

- 272 Levitus, S., J. I. Antonov, T. P. Boyer, O. K. Baranova, H. E. Garcia, R. A. Locarnini,  
273 A. V. Mishonov, J. R. Reagan, D. Seidov, E. S. Yarosh, and M. M. Zweng (2012), World  
274 ocean heat content and thermosteric sea level change (0-2000 m), 1955-2010, *Geophys.*  
275 *Res. Lett.*, *39*, L10,603.
- 276 Marshall, J., A. Adcroft, C. Hill, L. Perelman, and C. Heisey (1997), A finite-volume,  
277 incompressible Navier Stokes model for studies of the ocean on parallel computers, *J.*  
278 *Geophys. Res.*, *102*, 5753–5766.
- 279 Meijers, A. J. S., N. L. Bindoff, and S. R. Rintoul (2011), Frontal movements and property  
280 fluxes: Contributions to heat and freshwater trends in the Southern Ocean, *J. Geophys.*  
281 *Res.*, *116*, C08,024.
- 282 Meredith, M. P., and A. McC. Hogg (2006), Circumpolar response of Southern Ocean eddy  
283 activity to a change in the Southern Annular Mode, *Geophys. Res. Lett.*, *33*, L16,608.
- 284 Morrison, A. K., and A. McC. Hogg (2013), On the Relationship between Southern Ocean  
285 Overturning and ACC Transport, *J. Phys. Oceanogr.*, *43*, 140–148.
- 286 Redi, M. H. (1982), Oceanic isopycnal mixing by coordinate rotation, *J. Phys. Oceanogr.*,  
287 *12*, 1154–1158.
- 288 Thompson, D. W. J., and S. Solomon (2002), Interpretation of recent Southern Hemi-  
289 sphere climate change, *Science*, *296*, 895–899.
- 290 Wolfe, C. L., and P. Cessi (2009), Overturning circulation in an eddy-resolving model:  
291 The effect of the pole-to-pole temperature gradient, *J. Phys. Oceanogr.*, *39*, 125–142.
- 292 Wolfe, C. L., P. Cessi, J. L. McClean, and M. E. Maltrud (2008), Vertical heat transport  
293 in eddy ocean models, *Geophys. Res. Lett.*, *35*, L23,605.

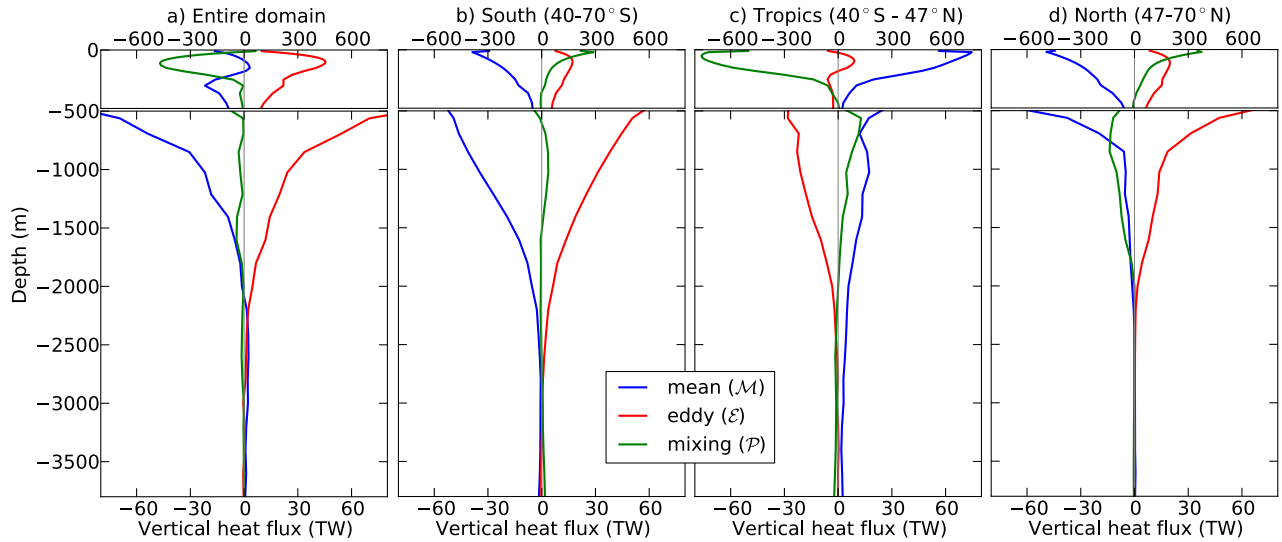


**Figure 1.** Vertical heat fluxes for the reference case, averaged over 10 years and different subdomains as follows: a) the entire model domain, b) the southern region ( $40\text{-}70^\circ\text{S}$ ), c) the tropics ( $40^\circ\text{S}\text{-}47^\circ\text{N}$ ), and d) the northern region ( $47\text{-}70^\circ\text{N}$ ). Note that the ‘vertical’ mean and eddy fluxes, as defined in Equations 3 and 4, represent the net divergence, including horizontal fluxes across the subdomain boundaries. Positive values indicate upward heat flux. Colours show the heat flux components as defined in Section 3, with ‘mixing’ being the sum of sub-gridscale fluxes including parameterised convection and turbulent diffusion. The heat content tendency ( $\mathcal{T}$ ; not shown) is negligible. The horizontal scale has been increased below 500 m to show detail at depth.



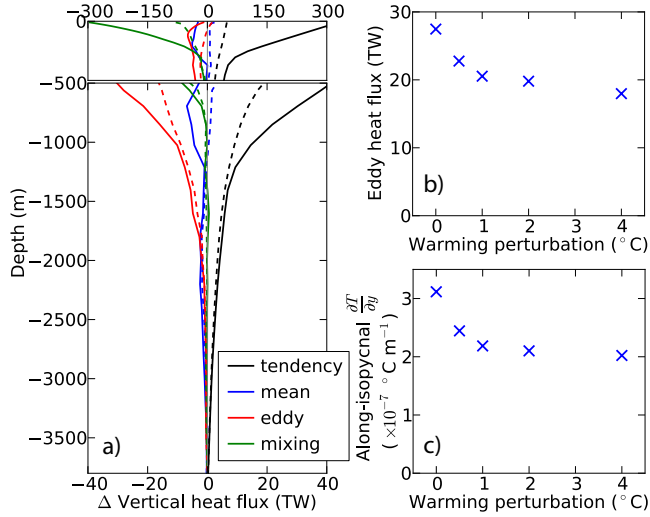


**Figure 2.** Vertical heat flux response to a uniform  $+2^\circ\text{C}$  warming perturbation. a) Change from the equilibrium vertical heat fluxes, averaged over the first ten years of the perturbation, integrated over the entire domain (solid lines) and the contribution from the southern region (dashed lines). Heat flux components (colours) are defined as in Figure 1, with the additional heat content tendency,  $\mathcal{T}$  (black). b) Scaling of the vertical eddy heat flux in the southern region (i.e. the blue line in Figure 1b), averaged over the depth range 700-1600 m. c) Scaling of the along-isopycnal, meridional temperature gradient on a mid-depth isopycnal (1500 m depth at  $42^\circ\text{S}$ , 700 m depth at  $62^\circ\text{S}$ ).

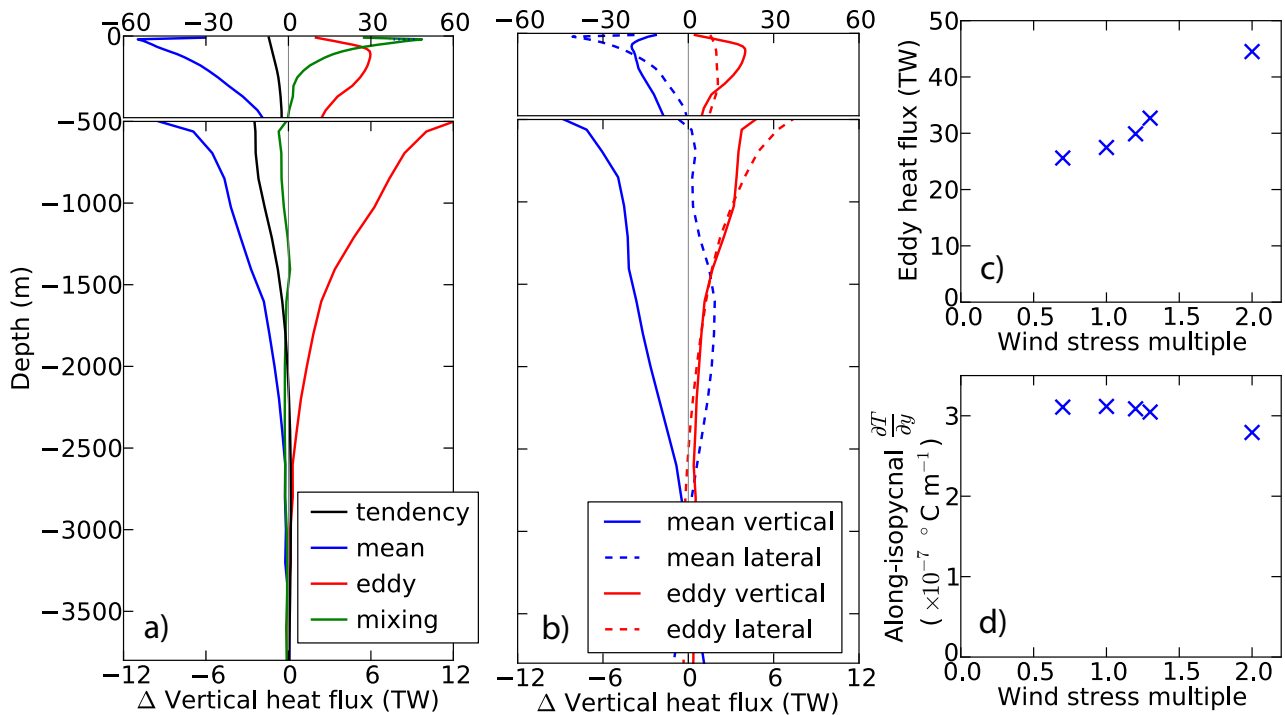


**Figure 3.** Heat flux response in the southern region (40-70°S only) to a 30% increase in Southern Ocean wind stress. a) Change from the equilibrium vertical heat fluxes (net heat divergence) in the southern region, averaged over the first ten years of the perturbation. Heat flux components (colours) are defined as in Figure 1, with the additional heat content tendency,  $\mathcal{T}$  (black). b) Separation of the net mean and eddy heat fluxes shown in a) into true vertical (solid lines) and lateral (dashed lines) components. c) Scaling of the net eddy heat flux in the southern region, averaged over the depth range 700-1600 m. d) Scaling of the along-isopycnal, meridional temperature gradient on a mid-depth isopycnal (1500 m depth at 42°S, 700 m depth at 62°S).